Moraine dam related to late Quaternary glaciation in the Yulong Mountains, southwest China, and impacts on the Jinsha River

Ping Kong [a,b,*], Chunguang Na [a], David Fink [c], Xitao Zhao [a], Wei Xiao [a]

[a] Key Laboratory of the Earth's Deep Interior, Institute of Geology and Geophysics, Chinese Academy of Sciences, P.O. Box 9825, Beijing 100029, China
[b] Institute of Tibetan Plateau Research, Chinese Academy of Sciences, Beijing 100085, China
[c] Institute for Environmental Research, Australian Nuclear Science & Technology Organisation, Menai, NSW 2234, Australia

A B S T R A C T

The Yulong Mountain massif is tectonically active during Quaternary and contains the southernmost glacierized mountains in China, and all of Eurasia. Past glacial remnants remain preserved on the east and west sides of the Yulong Mountains. A ridge of moraine protruded into the Jinsha River at the Daju Basin, damming the river, and forming a lake at the head of the Jinsha River. Cosmogenic ^{10}Be and ^{26}Al provide exposure age dates for the moraine-based fluvial terraces left behind after the dam breached, and for moraine boulders on both the eastern and western sides of the Yulong Mountains. Our results yield exposure ages for the terraces that range from 29 ka to 8 ka, and a downcutting rate of 7.6 m/ka. The preservation of the remaining dam for over 10,000 years suggests stability of the moraine dam and gradual erosion of the dam during drainage of the dammed lake. From the relationship between exposure ages and elevations of the fluvial terraces located in different walls of the Daju fault, we obtain a late Quaternary dip-slip rate of about 5.6 m/ka for the Daju fault. The exposure ages of 10.2 ka and 47 ka for moraine boulders located in the east and west sides of the Yulong Mountains, respectively, coincide with warm periods in the late Quaternary. This implies that precipitation provides the major control for glaciations on the Yulong Mountains, a domain of the southwest Asian monsoon.

© 2009 Elsevier Ltd. All rights reserved.

1. Introduction

Studies of cataclysmic floods after failure of ice- or moraine-dammed lakes call attention to such high-magnitude and low-frequency events on bedrock river incision, landscape evolution, and impacts of climatic fluctuations (Baker et al., 1993; Montgomery et al., 2004; Reuther et al., 2006; McKillop and Clague, 2007; Komatsu et al., 2009). Although many such studies focus on high-latitude regions, the effects from such catastrophic floods in tectonically active mountain ranges are particularly interesting where climatic, tectonic and erosional processes interact (Korup and Tweed, 2007; Korup and Montgomery, 2008). This paper reports the results of a study of the failure of a moraine dam related to late Quaternary glaciation of Yulong Mountains in the low-latitude intramontane basin, Daju Basin.

Located 25 km north of Lijiang, the south–north trending Yulong Mountain massif (27°03′–27°16′N, 100°07′–100°15′E) constitutes the southernmost glacierized mountains in Eurasia (Fig. 1). The Yulong Mountains have been tectonically active during the Quaternary, with mainly normal faults around the margins of the range. The Daju and Lijiang basins bound the northeast and southeast sides of the mountain range, and the Jinsha River flows past the west side of the mountains.

The east and west valleys of Yulong Mountains preserve relics of Pleistocene glaciations (Zhao et al., 1999, 2007a). A ridge of moraine-outwash along the east valley protruded into the Jinsha River, having blocked the river at the Daju basin. Some moraine-outwash may have also come from the neighboring Haba Mountains, and mixed within the Daju Basin. The moraine-outwash occupied the entire basin and the dam extended basin-wide, ∼3 × 4 km². The original shape of the moraine dam has now been destroyed, leaving moraine-based fluvial terraces at the Daju Basin. Upstream of Daju, more than a dozen outcrops of lacustrine deposits occur below 1900 m along the bank of the Jinsha River (Zhao et al., 2007b), indicating that a lake formed in this region.
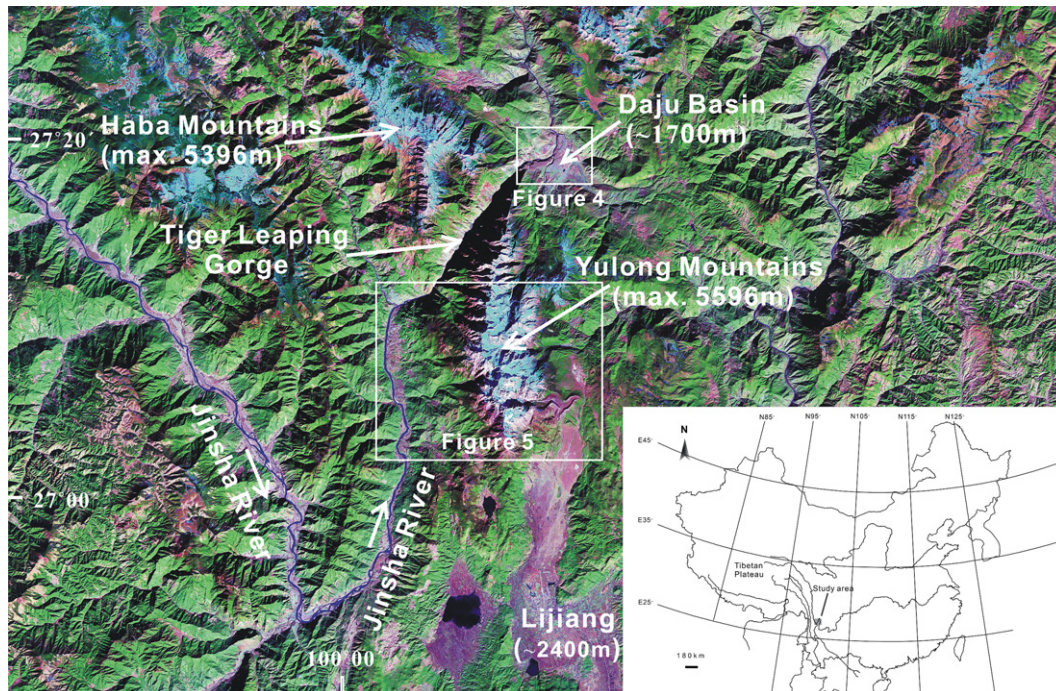
Fig. 1. Study areas around the Yulong Mountains. The south–north trending Yulong Mountain massif is the southernmost glacierized mountains in China and all of Eurasia. The Jinsha River forms an extremely narrow gorge, called 'tiger-leaping gorge', when passing through Yulong and Haba Mountains, with 3800 m of relief and with slopes of up to >60°. The DEM image is from Global Land Cover Facility.

Immediately upstream of Daju, the Yangtze River incises into bedrock, forming an extremely narrow gorge, called 'Tiger-leaping Gorge', with ~3800 m of relief, and at some portions >60° steep scarps. Since moraine dams may have occurred repeatedly at Daju and possibly also on the west side of the Yulong Mountains during the Quaternary, it is important to understand the degree to which outburst floods have affected the landscape in this region. Furthermore, the Yangtze River is one of the ten largest river systems in the world as measured by length, drainage area, sediment transport and water discharge; annual water discharge reaches ~950×10^9 m^3, ranking fifth in the world (Saito et al., 2001). Outburst floods after failure of moraine dams could severely threaten lives downstream and cause huge property loss. Thus, understanding the style of dam failure (catastrophic or gradual) in such an intramontane basin provides the basis for developing proper responses to future hazards.

This work intends to develop time constraints on formation of moraine-based fluvial terraces at the Daju Basin, past glaciations in the area around the Yulong Mountains and dip-slip rates of the Daju fault, using cosmogenic nuclide dating techniques. These time constraints will hopefully clarify the controls for glacier development in the sub-tropical area of the Yulong Mountains and improve our understanding of the failure of moraine dams in intramontane basins.

2. Geological setting and sampling

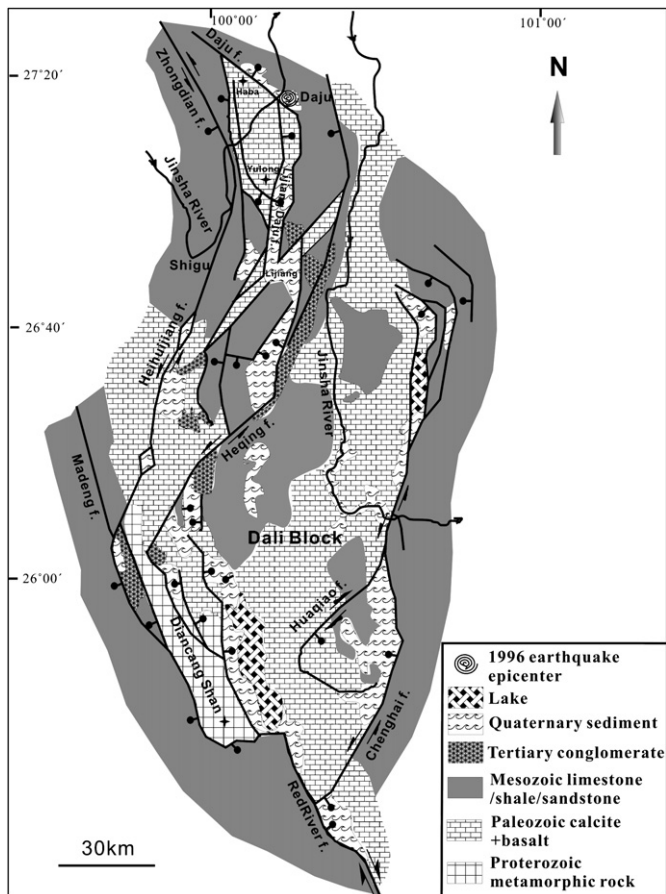### 2.1. Uplift of the Yulong Mountains vs downcutting of the Jinsha River

A closed network of active transtensional faults defines the Yulong Mountain range (Fig. 2). Steeply dipping Quaternary faults bound the Yulong Mountains on the east and north, and between Lijiang and Daju these faults appear to be mostly normal with roughly N–S strikes (Lacassin et al., 1996). The most recent rupture of the Lijiang–Daju fault led to a magnitude 7.0 quake at Lijiang in 1996 (Han et al., 2004). The epicenter of the earthquake lies at the Daju Basin. The steep mountain hillslopes at the bounding faults frequently experience large-magnitude landslides. The Jinsha River passing through the west of the Yulong Mountains becomes extremely narrow and exceptionally steep, suggesting adjustment to high rates of surface uplift.

Based on ^{39}Ar/^{40}Ar dating of K-feldspar in the core of the Yulong Mountains, Lacassin et al. (1996) suggested that the uplift of the mountains occurred by antiformal folding around 17 Ma, as Indochina's extrusion came to an end. Based on stratigraphic relationships, Fan et al. (2006) inferred that at least 3000 m of normal displacement occurred along the Lijiang–Daju fault (in their definition, it is called the northern segment of the Heqing fault), resulting in the relative uplift of the Yulong Mountain massif. The initiation of the Heqing fault is believed to have taken place 2.78 Ma ago (Xiao et al., 2006, 2007). Studying apatite and zircon-fission track ages, Han et al. (2004) suggested that activity on the Lijiang–Daju fault began at the beginning of the Quaternary.

The Daju fault, bounding the Yulong Mountains on the north, also displays active dip-slip features (Fig. 3A). This activity led to formation of the small intramontane Daju Basin (Fig. 3B). Fan et al. (2006) interpreted the Daju fault as the northwestern continuation of the northern segment of the Heqing fault. Wu et al. (2008) suggested that the Haba–Daju–Lijiang fault is a continuous, independent fault which bends at Daju.

Quaternary deposits 100–200 m thick fill the Daju Basin. The Jinsha River passes through the basin, leaving fluvial terraces conspicuous on DEM images and in the field (Figs. 3C and 4). The highest terrace at the Daju Basin sites at ~1900 m. Upstream of Daju, more than a dozen outcrops of lacustrine deposits can be seen on the bank of the Jinsha River near the first bend of the Yangtze River at Shigu (Fig. 3E). All the lacustrine deposits occur below 1900 m, suggesting that the deposits at Daju dammed the Jinsha River. The time-scale of the fluvial terraces at Daju reflect the stability of the dam and the style of dam failure.

Fig. 2. Geologic map of the Dali region and vicinity. The Yulong Mountain range is defined by a closed network of active transtensional faults. Steeply dipping Quaternary faults, on the east and north bounds of the Yulong Mountains, appear to be mostly normal and strike roughly N–S between Lijiang and Daju. After Fan et al. (2006).

The northern part of the Yulong Mountain range consists of Carboniferous and Devonian limestones. The glacierized peaks and the southern spur overlie Permian basalt, Triassic limestone and shale (Ives and Zhang, 1993). As the Quaternary deposits at Daju include basalt as a component, the deposits cannot form by erosion of surrounding mountains due to tectonic deformation; they must have been delivered from the glacierized area of the Yulong Mountains. Zhao et al, (2006) interpreted the upper diamict deposits at Daju as outwash delivered from the Yulong and Haba Mountains, based on the tilt of the strata. Zheng (2000) suggested the deposits at Daju may have been delivered by mud flow. Because the upper deposits, consist of poorly sorted diamicton, contain angular clasts with sharp edges, and lack stratification or vertical grading of particle sizes, we prefer an interpretation of till and of glacial origin. Meter to tens of meters sized boulders are widespread and embedded in the terraces. The boulders mostly consist of limestone, but a few are basalt (Fig. 3C). We sampled quartz occurring in veins at the top of the boulders within the fluvial terrace profile (Fig. 3F). Fig. 4 indicates the sample locations.

2.2. Glaciations on the Yulong Mountains

Eighteen peaks rise above 5000 m asl within the Yulong Mountain range, with the highest peak measuring 5596 m asl. These contain 19 modern glaciers covering an area of 11.61 km^2, among which 15 are in the east side and four are in the west side

(Pang et al., 2006). The largest glacier, the Baishui Glacier No. 1 located on the east slope of the Yulong Mountains, has retreated 75 m during the past 5 years from 2001 to 2006 (Ning et al., 2006).

The southwest Asian monsoon controls the climates at Mount Yulong, lying on, in a large scale, the southern end of the Hengduan mountain range. According to the records of the Lijiang Meteorological Station at 2393 m, the annual temperature averages ∼12.6 °C and annual precipitation averages ∼1000 mm (He et al., 2002; Zhang et al., 2007). Equilibrium snow lines lie at ∼4800 m around the Yulong Mountains, the annual temperature at this elevation averages about −3.3 °C (He et al., 2002) and annual precipitation may reach 2000 mm (Zhang et al., 2004). Large accumulations and ablation, high temperatures, intense melting, and rapid movement characterize the glaciers on the Yulong Mountains, resulting in high sensitivity to climate change, typical of temperate glaciers.

Table 1 summarizes the previous identification of moraines and classification of the glaciations around the Yulong Mountains. The glacial moraines distributed along the east side of the Yulong Mountains have been relatively well studied. Some authors believed them to be remnants of the most recent glacial advances (Jen, 1958; Huang, 1960; Ives and Zhang, 1993). Others have classified at least three stages of glacial advance (Ming, 1996; Zhao et al., 1999; Zheng, 2000). Zhao et al. (1999, 2007a) dated the moraines in the east and west valleys of the Yulong Mountains using electron spin resonance (ESR). They suggested dates for four glaciations consistently recorded in both the eastern and western valleys: 700–600 ka, 530–450 ka, 310–130 ka, and 24–18 ka. Ming (1996) and Zhao et al. (1999) suggest that the moraine at the Daju basin and two 100 m high ridges perpendicularly intersect with Ganheba where we collected samples YN-64 and YN-65 (Figs. 5 and 6) represent remnants of the earliest glacial retreat preserved at the east side, 0.6–0.7 Ma ago. Ming (1996) and Zhao et al. (1999) further identified moraines at the area of Ganhaizi where we collected samples YN-62 and YN-63 as relics of glacial retreat ∼0.5 Ma ago.

Among the 19 modern glaciers within the Yulong Mountains, four lie on the western slope, and their extents are much less than those on the eastern slope. Differing from those on the east side of the mountains, moraines on the west side lie mostly within the Xinlian, Zhongyi and Renhe valleys (Fig. 5). The state of the relic deposits make it difficult to judge whether the moraine ridges that developed on the west side of the Yulong Mountains have protruded into the Jinsha River, since some diamict deposits along the Jinsha River west of the mountains may have originated through mass wasting (Liu et al., 2005). Zhao et al. (2007a) recognized four stages of glacial advance, similar to those on the east side. They suggest that the moraine where we collected samples of YN-52 to YN-56 belongs to the earliest glacial remnant. According to their classification, our sample YN-50 would be a relic of a glacial retreat 0.31–0.13 Ma ago, whereas our sample YN-48 would be a relic of a glacial retreat during the last glacial period.

The meter-size moraine boulders consist mostly of limestone, with a few of basalt, similar to those on the east side. We sampled the quartz veins exposed at the top of meter-size boulders to determine exposure ages. As quartz veins occur in only a few boulders, we cannot use ^{10}Be and ^{26}Al to systematically date moraine sequences on both sides of the Yulong Mountains.

3. Methodology

We have collected 14 samples from boulders embedded in the fluvial terraces at the Daju Basin to study the incision rate of the Jinsha River related to drainage of the dammed lake, through dating cosmogenic nuclide exposure ages of the boulders. We have also collected 11 samples from moraine boulders representative of past glaciations around the Yulong Mountains. All samples were taken
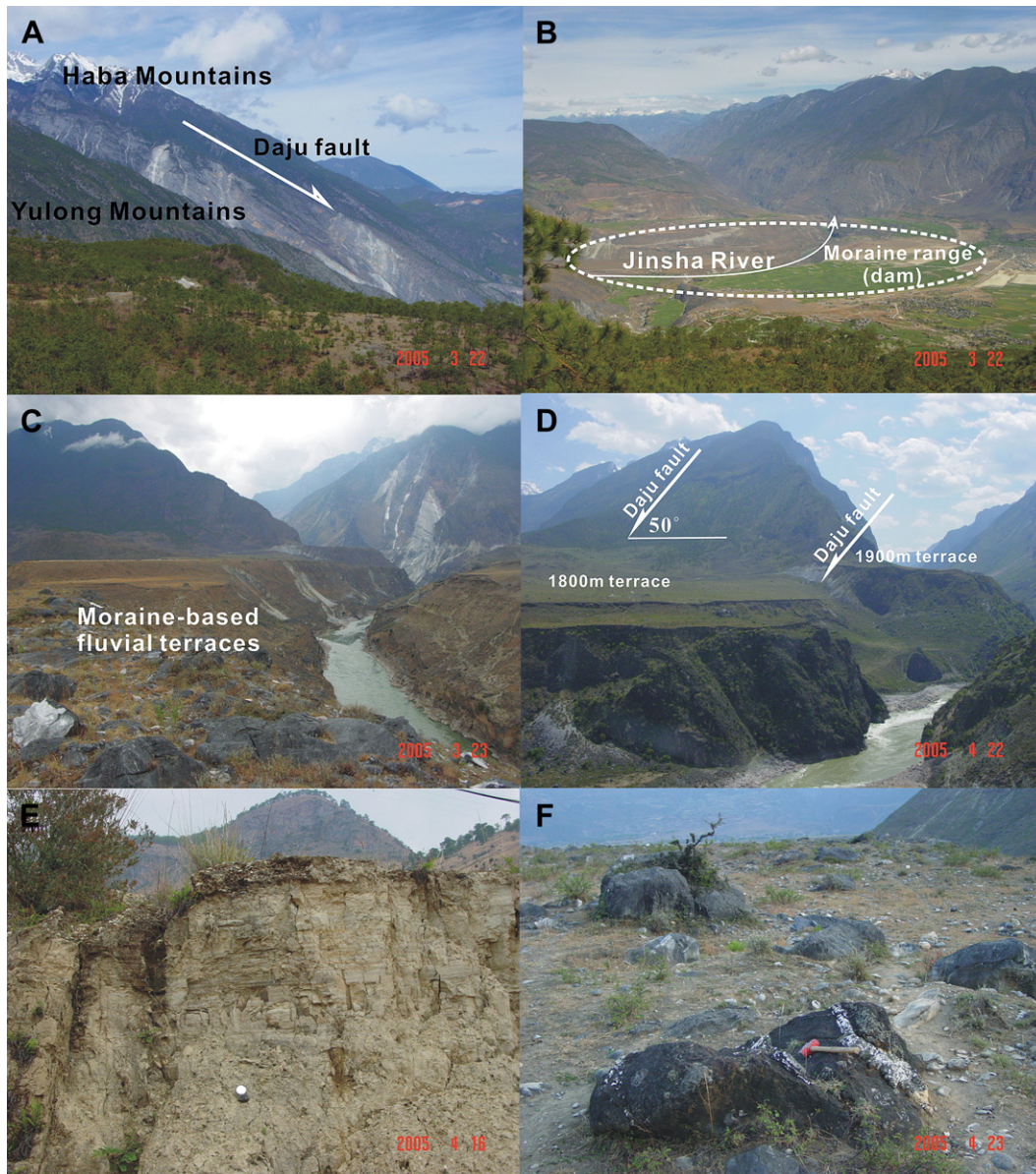
Fig. 3. Photographs taken for the Daju Basin and its upstream areas. (A) Daju normal fault along the Yulong and Haba Mountains. The Jinsha River passes through between these two mountains; (B) well-preserved moraine-based fluvial terraces at the Daju Basin. Dashed line shows the range of the moraine dam; (C) boulders of meter to tens meter-size are widespread and embedded in the fluvial terraces, which mostly consist of limestone, with a few of basalt; (D) a normal fault scarp formed between the highest terrace and the next terrace. The highest terrace sits on the footwall of the Daju fault, whereas the other terraces are situated on the hanging wall of the normal fault; (E) Lacustrine sediments occurring on the bank of the Jinsha River near Shigu, the first bend of the Yangtze River. The white spot in the lower middle is a compass; (F) boulders with quartz veins protrude out of the basal limestone or basalt rocks.

from quartz veins exposed at the upper surfaces of limestone or basalt boulders of >1 m diameter, with sample thickness in all cases being ≤3 cm. We made geometric corrections for horizon shielding of the cosmic ray flux based on the method of Dunne et al. (1999).

Chemical preparations, from extraction of quartz to final oxide, were carried out at the cosmogenic nuclide laboratory in the Institute of Geology and Geophysics, Chinese Academy of Sciences, in Beijing. Samples were first crushed to 0.1 ∼ 1.0 mm size. Meteoric ^{10}Be was removed by repeat ultrasonic leaching at 80 °C with a mixed solution of dilute HF and HNO$_3$ (Kohl and Nishiizumi, 1992). Pure quartz samples were subsequently dissolved with addition of ∼0.6 mg ^{9}Be carrier. Be and Al were progressively separated by anion exchange, acetyl acetone-CCl$_4$ extraction, cation

exchange and selective precipitation, and finally converted to oxide.

The oxides were mixed with niobium metal powder and both ^{10}Be and ^{26}Al concentrations were measured by accelerator mass spectrometry (AMS) at the ANTARES AMS facility of the Australian Nuclear Science & Technology Organisation (Fink and Smith, 2007). Measured ratios of ^{10}Be/^{9}Be were normalized relative to the NIST standard, SRM-4325, with the certified isotopic ratio of 2.68×10^{-11}. Correspondingly we use half lives of 1.34 Ma and 0.71 Ma for ^{10}Be and ^{26}Al, respectively. Recent studies favor the 1.34 Ma half-life for ^{10}Be (Fink and Smith, 2007; Nishiizumi et al., 2007). Using the different half-life of 1.51 Ma, together with the high-latitude, sea-level production rate of 5.1 for ^{10}Be, would alter exposure ages by less than 1%. All measured ratios were corrected
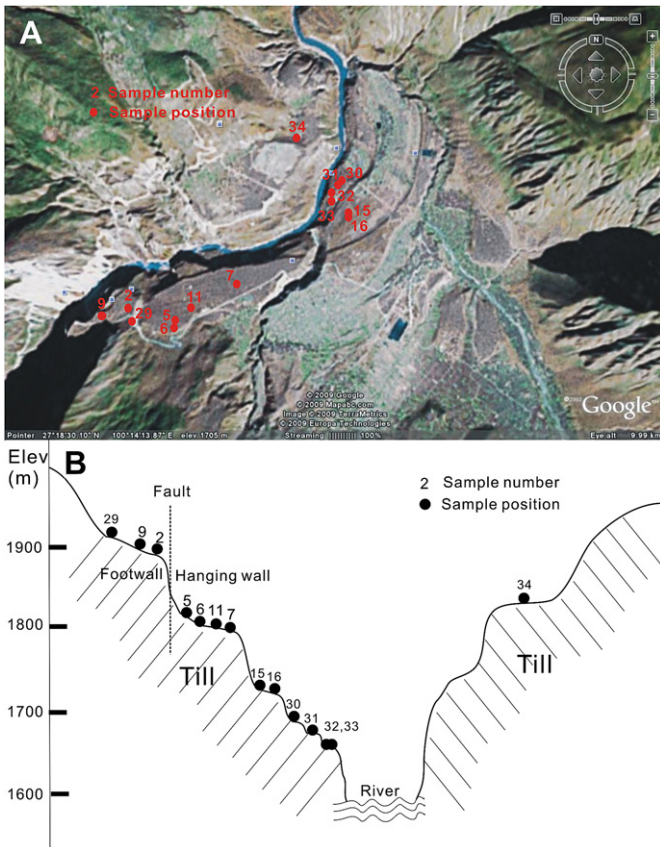
Fig. 4. Samples collected from moraine-based fluvial terraces at the Daju Basin. Quartz veins exposed at the top of the moraine boulders were taken for cosmogenic nuclide exposure dating. Sample information and related exposure ages are given in Table 2. (A) Sample positions at the Daju Basin. The image is from 'google earth'; (B) plot of sample positions vs sample elevations.

for the ^{10}Be/^{9}Be ratios of chemical procedure blanks which ranged in value of $(5–8) \times 10^{-15}$.

Production rates of cosmogenic nuclides at the Earth's surface vary with latitude and elevation. We calculate site-specific production rates using scaling factors based on the methods of Stone

(2000). The resultant scaling factors are combined with the high-latitude, sea-level production rate of 4.5 atoms/g.quartz/years for ^{10}Be and 31.1 atoms/g.quartz/years for ^{26}Al. We assume a contribution of 2.5% production by muons at sea-level. Final site-specific production rates for all samples include geometric corrections for horizon shielding of the cosmic ray flux and geomagnetic intensity variation corrections according to the method of Dunai (2001), and a correction for a 2–3 cm sample thickness. Using the different scaling methods of Dunai (2000), Lifton et al. (2005), or Desilets et al. (2006) can increase the calculated exposure ages by a maximum of 5% (for old exposure ages) to 10% (for young exposure ages).

4. Results

Table 2 gives ^{10}Be and ^{26}Al exposure ages for boulders embedded in the fluvial terraces and Table 3 shows the calculated ages for boulders related to past glaciations around the Yulong Mountains. Although the obtained exposure ages all apply to moraine boulders, they reflect different geologic events. The exposure ages for boulders embedded in the fluvial terraces do not reflect glacial advances or retreats, as most probably they were preserved inside the moraine ridge during glacial advances, and they were exposed by the removal of the upper part of the moraine ridge by stream erosion. Thus, the exposure ages most likely reflect the formation time of the fluvial terraces.

Moreover we have to consider several other factors that may complicate the linkage between cosmogenic nuclide exposure age and the time of fluvial terrace formation or boulder deposition as follows.

(1) Complex exposures: inheritance occurs when a rock fails to lose the cosmogenic nuclide concentration acquired prior to transport by glacier ice. For boulders within the fluvial terraces, another possibility exists for complex exposure: the boulders could have been at the top of the moraine ridge and exposed before the fluvial terrace formation. This would result in exposure ages older than the time of boulder deposition or terrace formation. Analysis of boulder ages published in the literature indicates that <3% of all moraine boulders have prior exposure (Putkonen and Swanson, 2003). Thus if complex exposure occurs, we may expect one boulder has an exposure age significantly older than other parallel samples. Our data do not show such a case occurred in our samples. One more method to judge if a sample has complex exposure

Table 1
Previous identification of moraines and classification of glaciations around the Yulong Mountains.

| Glaciation stage	I	II	III	IV
References	Dali glaciation	Lijiang glaciation	Ganhaizi glaciation	Jinsha glaciation
East side				
Jen (1958) Huang (1960)	Ganheba, Ma Huang Pa (late Würm)	A-Li-Li-Chu (south of Fig. 5)		
Ives and Zhang (1993)	Ganheba, Ma Huang Pa (25,000–18,000 years?)	No identification (early Würm?)		
Ming (1996)	Ganheba	Baishui	Ganhaizi, two ridges perpendicular Ganheba (mid-Pleistocene)	Daju (early Pleistocene)
Zhao et al. (1999)	Ganheba	Baishui (0.31–0.13 Ma, ESR age)	Ganhaizi (0.53–0.45 Ma, ESR age)	two ridges perpendicular Ganheba (0.7–0.6 Ma, ESR age)
Zheng (2000)	Ganheba, Ma Huang Pa (24,000 years)	Baishui	Ganhaizi	
West side				
Zhao et al. (2007)	First inner lateral moraine in Xinlian, Zhongyi and Renhe valleys	Second inner lateral moraine in Xinlian, Zhongyi and Renhe valleys	Some part in Xinlian and Zhongyi valleys	Yankeyu in Xinlian valley, south of Renhe valley
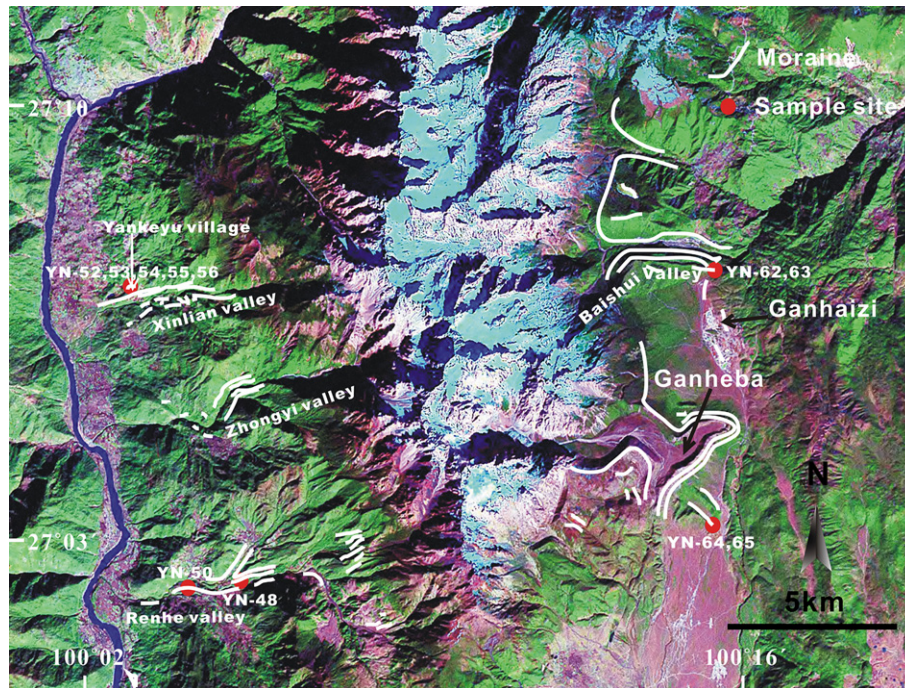
Fig. 5. Relic moraines of past glaciations preserved in the east and west sides of the Yulong Mountains with positions of our collected samples for exposure age dating. Sample information and related exposure ages are given in Table 3. The DEM image is from Global Land Cover Facility.

history is to plot the ^{26}Al/^{10}Be ratio vs ^{10}Be concentration for the sample in an erosion island diagram. In the diagram, one line represents changes of concentration ratios of two nuclides with time assuming no erosion; the other line represents changes of concentration ratios of two nuclides with time for various erosion rates. The two lines form a closed island, called the erosion island (Lal, 1991). Located within the island, the sample has experienced constant exposure; otherwise the sample has a complex exposure history or a complicated chemical composition. Fig. 7 shows plots of the ^{26}Al/^{10}Be ratios vs ^{10}Be concentrations for all our samples. The data basically lie within the erosion island, although some points are slightly offset from the steady state erosion line. This can result because at an early stage, ^{27}Al concentrations were measured after the HF medium was converted to HCl medium at the cosmogenic nuclide laboratory in the institute of Geology and Geophysics, Chinese Academy of Sciences. This step likely leads to an underestimation of ^{27}Al concentrations by 10–15% in samples with high Al contents. Thus, with a ^{26}Al/^{27}Al ratio given by AMS determination, ^{26}Al concentrations are also likely to be underestimated at a similar level. This problem has been resolved in our latter sample preparations (Kong et al., 2009a). For samples in this study, the consistent exposure ages for boulders at a similar location and the plots of ^{26}Al/^{10}Be ratios vs ^{10}Be concentrations suggest that these samples have not experienced detectable complex exposure histories.

Erosion: if not adequately considered, erosion of boulders leads to underestimation of exposure ages. Most of our sampled boulders do show significant erosion of limestone, leading quartz veins to extend out of the surfaces of boulders. Owen et al. (2002) estimated 1–5 mm/ka erosion rates for granitic boulders from the Hunza Valley, Karakoram Mountains. Kaplan et al. (2005) obtained an average erosion rate of 1.4 mm/ka for granitic boulders at Lago Buenos Aires, Argentina. Although the semi-arid climate settings reported by Owen et al. (2002) and Kaplan et al. (2005) differ from that related with the Yulong Mountains in southwest China, previous studies (Riebe et al., 2001; Kong et al., 2007) show that

climate shift is not a key control of erosion rate. As quartz resists erosion better than granite, we take 1 mm/ka as an erosion rate for quartz veins to see to what degree it affects exposure ages. Introducing erosion rates of 1 mm/ka increases calculated 10 ka exposure ages by 2%, and 50 ka exposure ages by 5%, which are within the uncertainties related to the production rate.

Sample over-turning or post-depositional cover: if not considered, these processes can lead to younger exposure ages. Our samples have stable geomorphic positions, and most of the boulders are partly embedded within the deposits. Therefore these samples are not likely to have experienced post-depositional sliding or turning of the boulders. Furthermore, our samples lie at elevations from 1660 m to 3070 m. Hence, they are not likely to have been covered by later glaciers or by seasonal snow.

Considering all the above factors, we believe the ^{10}Be and ^{26}Al ages we obtained to be representative of terrace formation ages for samples listed in Table 2 and depositional ages of boulders in Table 3.

For the two highest terraces, Table 2 shows unexpected younger exposure ages for the higher terrace and older exposure ages for the lower terrace. This results from the highest terrace being situated on the footwall of the Daju fault, whereas the other terraces are situated on the hanging wall of the normal fault (Figs. 3D and 4B). From Fig. 3D one can see a normal-fault scarp formed between the highest terrace and the next terrace. Wu et al. (2008) identified the fault scarp as the turning point of the Haba–Daju–Lijiang fault. Fig. 8A shows the plot of elevations vs exposure ages for the hanging wall terrace boulders. The virtually linear relationship between elevation and exposure age suggests a constant rate of downcutting of the moraine dam by the Jinsha River during drainage of the dammed lake.

The exposure ages of the five oldest moraine boulders on the west side of the Yulong Mountains, YN-52–YN-56, all fall within Marine Isotope stage-3 (MIS-3, 30–60 ka), with an average age of 47 ka. The other two samples on the west side of the Yulong Mountains, YN-48 and YN-50, yield ages much younger than previously proposed by Zhao et al. (2007a), although in the correct
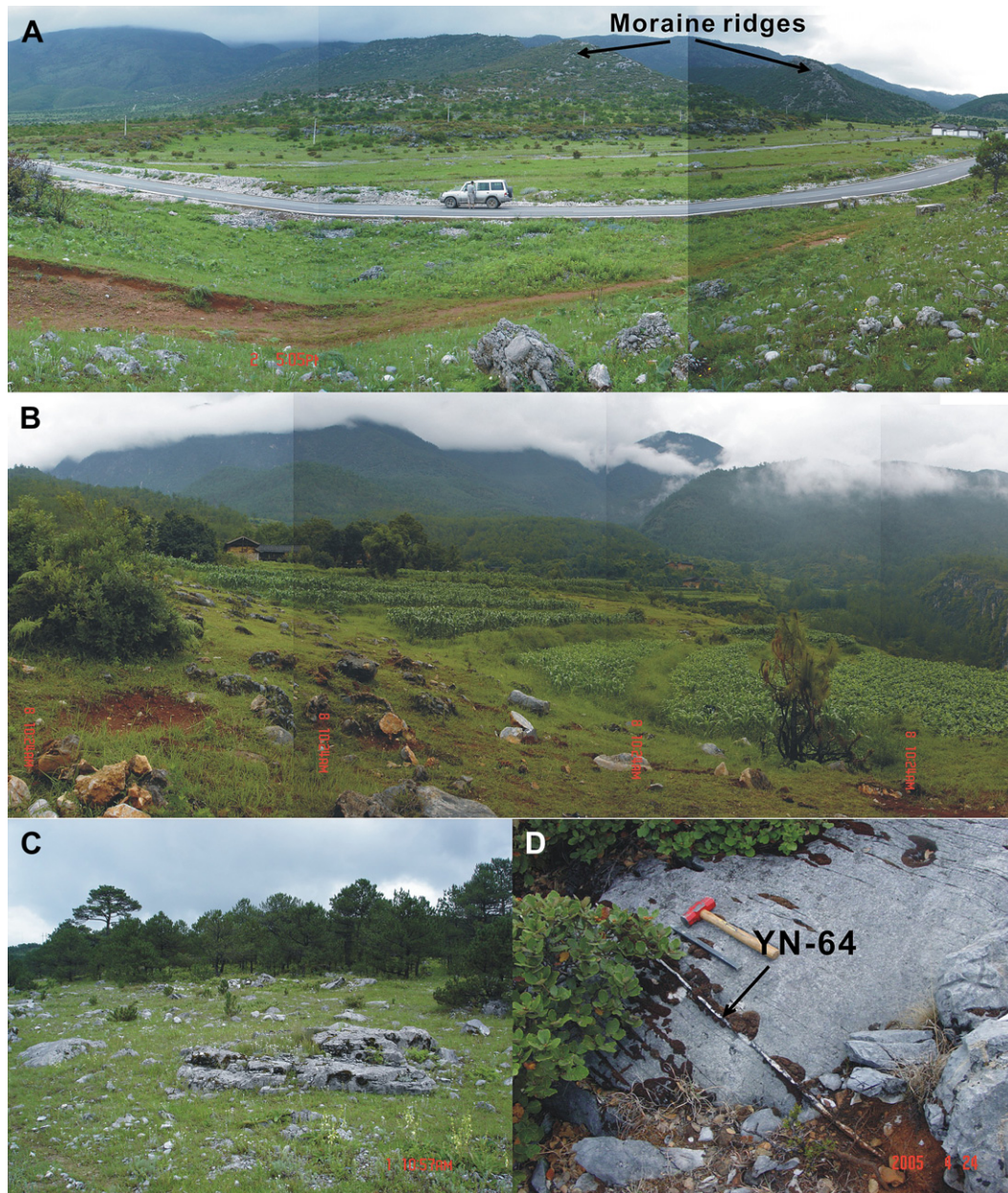
Fig. 6. Photos for moraine ridges preserved in the east and west sides of the Yulong Mountains. (A) Two 100 m high moraine ridges perpendicularly intersecting with Ganheba, on the east side of the Yulong Mountains; (B) moraine at Yankeyu, the oldest glacial relics preserved in the west side of the Yulong Mountains where we collected samples YN-52–YN-56; (C) moraine at Ganhaizi, on the east side of the Yulong Mountains; (D) due to differential erosion, the quartz vein protrudes out of the basal limestone rock.

stratigraphic sequence. The four samples from the east side of the Yulong Mountains, which Zhao et al. (1999) believed to represent the oldest moraines on the east side, have similar exposure ages, from 8.9 ka to 11.3 ka with an average of 10.2 ka. We have not found boulders with exposure ages within MIS-3 on the east side.

5. Discussions

5.1. Dip-slip rate of the Daju fault

From the linear relationship between elevation and exposure age for the hanging wall terrace samples, we can calculate the vertical offset of the footwall after the terrace formation. As YN-34 lies on the other side of the river, we do not include this sample in the calculation. The average exposure age of the footwall boulders

is 23.3 ka. Putting the age into the relationship between elevation and exposure age for the hanging wall samples, we obtain an elevation of 1770 m for the footwall terrace when it was formed. This leads to a vertical uplift of 130 m during the period of 23.3 ka, thus giving a dip-slip rate of ~5.6 m/ka. This value matches our direct dating of the scarp (~6.5 m/ka, unpublished data of Kong). With the dip angle of the Daju fault (Fig. 3D), we calculate a slip rate of the Daju fault of ~7.3 m/ka.

The Jinsha River becomes extremely narrow and the slopes west of the Yulong Mountains are steep, with ~3800 m of relief and some sidewalls exceed 60° in slope. The steep slopes suggest that the mountains are tectonically active. This observation is consistent with the high slip rate we obtained for the Daju fault.

Based on vertical offsets of a flat platform within the hanging wall relative to the levels of two planation surfaces across the

Table 2
Exposure ages for Daju fluvial terrace samples.

Sample	Latitude (N)	Longitude (E)	Elev. (m)	Shielding	^{10}Be (10^5 atoms g^{-1})	^{26}Al (10^5 atoms g^{-1})	^{26}Al/^{10}Be	LC[a]	T (^{10}Be) (ka)	T (^{26}Al) (ka)	T (aver.) (ka)	T (corr.)[b] (ka)
Highest												
YN-2	27°17.83	100°12.40	1875	0.97	2.90 ± 0.06	18.2 ± 0.7	6.28	2.96	23.0 ± 1.5	21.0 ± 1.6	22.0 ± 1.6	21.2 ± 1.5
YN-9	27°17.75	100°12.21	1885	0.94	3.63 ± 0.28	23.4 ± 1.3	6.47	2.98	29.6 ± 2.3	27.9 ± 2.5	28.7 ± 2.4	26.8 ± 2.2
YN-29	27°17.71	100°12.42	1940	0.97	3.12 ± 0.07	19.6 ± 1.4	6.27	3.09	23.7 ± 1.5	21.6 ± 2.1	22.7 ± 1.8	21.8 ± 1.7
YN-34	27°19.10	100°13.90	1830	0.97	2.48 ± 0.05	16.5 ± 0.9	6.66	2.87	20.3 ± 1.3	19.7 ± 1.7	20.0 ± 1.5	19.4 ± 1.5
Second												
YN-5	27°17.69	100°12.84	1813	0.97	3.53 ± 0.18	22.6 ± 0.6	6.39	2.84	29.3 ± 2.3	27.2 ± 2.0	28.3 ± 2.2	26.4 ± 2.1
YN-6	27°17.69	100°12.84	1813	0.97	3.79 ± 0.13	23.4 ± 1.3	6.18	2.84	31.4 ± 2.2	28.3 ± 2.4	29.9 ± 2.3	27.9 ± 2.1
YN-7	27°17.97	100°13.46	1790	0.97	3.93 ± 0.10	22.4 ± 3.8	5.70	2.74	33.8 ± 2.2	28.1 ± 5.1	31.0 ± 3.7	28.7 ± 3.4
YN-11	27°17.70	100°12.96	1806	0.97	3.60 ± 0.16	25.7 ± 0.7	7.14	2.82	30.0 ± 2.2	31.3 ± 2.2	30.7 ± 2.2	28.4 ± 2.0
Third												
YN-15	27°18.50	100°14.28	1725	0.96	2.08 ± 0.05	13.8 ± 0.7	6.63	2.68	18.5 ± 1.2	17.8 ± 1.5	18.2 ± 1.4	17.7 ± 1.4
YN-16	27°18.50	100°14.28	1725	0.96	2.30 ± 0.11	14.5 ± 0.4	6.33	2.68	20.4 ± 1.5	18.8 ± 1.4	19.6 ± 1.5	19.0 ± 1.5
Fourth												
YN-30	27°18.78	100°14.27	1680	0.95	1.31 ± 0.06	7.8 ± 1.6	5.98	2.60	12.1 ± 1.0	10.5 ± 2.1	11.3 ± 1.6	11.3 ± 1.6
Fifth												
YN-31	27°18.78	100°14.27	1670	0.95	1.00 ± 0.06	6.7 ± 0.7	6.73	2.58	9.25 ± 0.78	9.0 ± 1.1	9.1 ± 1.0	9.1 ± 1.0
Sixth												
YN-32	27°18.78	100°14.27	1660	0.95	0.923 ± 0.03	5.71 ± 0.5	6.18	2.56	8.62 ± 0.59	7.7 ± 0.8	8.2 ± 0.7	8.3 ± 0.7
YN-33	27°18.78	100°14.27	1660	0.95	0.808 ± 0.02	n.d.		2.56	7.5 ± 1.0		7.5 ± 1.0	7.6 ± 1.0

The ^{10}Be and ^{26}Al exposure ages are calculated using scaling factors from Stone (2000). The errors with exposure ages also include 6% from production rate and 3% from ICP-OES for Al.

[a] Latitude & elevation correction.
[b] Ages corrected for geomagnetic intensity variations.

Yulong–Haba Mountain range, Han et al., (2004) estimated an average vertical slip rate for the Lijiang–Daju fault of 0.7 m/ka for the entire Quaternary and 1.69 m/ka since the mid-Pleistocene. These estimates would imply an increasing dip-slip rate and increasing tectonic activity with time for the Lijiang–Daju normal fault. The high slip rate also raises caution that large-magnitude earthquakes may frequently occur along the fault. Earthquakes occurring in China exhibit, on average, surface displacements of less than 1 m for M 7.0 quakes, and 5–10 m for M 8.0 quakes (Ma and Peng, 2006). This would imply possible earthquake recurrences along the Liang–Daju fault of more than seven M 7.0 quakes or between one or two M 8.0 quakes every thousand years.

5.2. Stability of the moraine dam

From the relationship between fluvial terrace exposure ages and their elevations (Fig. 8) we obtain a 7.6 m/ka average downcutting rate of the moraine dam. The strikingly linear relationship implies that the stream power remained rather constant during drainage of the lake. This value is comparable with the high incision rates of 1–12 m/ka for the high-relief Indus River in northern Pakistan (Burbank et al., 1996; Leland et al., 1998).

Moraine-dammed lakes usually form in response to glacial downwasting during an interglacial period, following earlier glacial advances (Korup and Tweed, 2007). The question is 'when did the moraine dam form at the Daju Basin?'. Dating the lacustrine sediments upstream of Daju provides one approach. Zhao et al. (2007b) studied these sediments using ESR, thermoluminescence (TL) and U-series disequilibrium methods. They have dated seven lacustrine sediment samples upstream of Daju using the TL technique and their ages range from 77 ka to 210 ka. Their U-series method for 3 different samples yields ages of 137 ka, 149 ka and 181 ka. They have also dated one sample via ESR, which gives an age of 243 ka; but the same sample yielded a TL age of 152 ka. The large range of

Table 3
Exposure ages for moraine boulders around the Yulong Mountains.

Sample	Latitude (N)	Longitude (E)	Elev. (m)	Shielding	^{10}Be ($\times 10^5$ atoms/g)	^{26}Al ($\times 10^5$ atoms/g)	^{26}Al/^{10}Be	LC[a]	T (^{10}Be) (ka)	T (^{26}Al) (ka)	T (aver.) (ka)	T (corr.)[b] (ka)
YN-48	27°02.30	100°06.82	2440	0.99	0.236 ± 0.024	1.64 ± 0.13	6.95	4.26	1.27 ± 0.14	1.28 ± 0.13	1.28 ± 0.14	1.35 ± 0.15
YN-50	27°02.28	100°05.84	2210	0.99	3.02 ± 0.06	7.7 ± 3.5	2.6	3.68	18.9 ± 1.2	7.0 ± 3.1	18.9 ± 1.2[c]	18.3 ± 1.2
YN-52	27°06.92	100°04.80	2240	0.99	8.04 ± 0.28	60.1 ± 1.8	7.47	3.76	49.6 ± 3.4	54.4 ± 4.0	52.0 ± 3.7	46.4 ± 3.3
YN-53	27°06.92	100°04.80	2240	0.99	9.87 ± 0.18	66.2 ± 3.0	6.72	3.76	61.1 ± 3.8	60.1 ± 4.8	60.6 ± 4.3	54.1 ± 3.8
YN-54	27°06.95	100°04.76	2250	0.99	6.25 ± 0.22	39.3 ± 2.4	6.29	3.78	38.2 ± 2.7	35.0 ± 3.2	36.6 ± 3.0	33.3 ± 2.7
YN-55	27°06.95	100°04.76	2250	0.99	9.28 ± 0.18	57.7 ± 1.2	6.22	3.78	57.0 ± 3.6	51.9 ± 3.6	54.4 ± 3.6	48.6 ± 3.2
YN-56	27°06.95	100°04.76	2250	0.99	7.94 ± 0.20	49.4 ± 2.0	6.23	3.78	48.6 ± 3.2	44.2 ± 3.4	46.4 ± 3.3	41.1 ± 2.9
YN-62	27°07.30	100°15.28	3070	1.00	3.27 ± 0.20	20.2 ± 1.6	6.16	6.24	11.9 ± 1.0	10.7 ± 1.1	11.3 ± 1.1	11.3 ± 1.1
YN-63	27°07.31	100°15.26	3060	1.00	2.76 ± 0.20	21.0 ± 1.8	7.63	6.20	10.1 ± 0.9	11.2 ± 1.2	10.7 ± 1.1	10.7 ± 1.1
YN-64	27°03.14	100°15.33	2930	1.00	2.21 ± 0.08	15.4 ± 2.3	6.98	5.75	8.71 ± 0.61	8.8 ± 1.4	8.8 ± 1.0	8.9 ± 1.0
YN-65	27°03.18	100°15.26	2960	1.00	2.91 ± 0.10	17.0 ± 5.8	5.84	5.85	11.3 ± 0.8	9.6 ± 3.3	10.5 ± 2.1	10.5 ± 2.1

The ^{10}Be and ^{26}Al exposure ages are calculated using scaling factors from Stone (2000). The errors with exposure ages also include 6% from production rate and 3% from ICP-OES for Al.

[a] Latitude & elevation correction.
[b] Ages corrected for geomagnetic intensity variations.
[c] The ^{10}Be exposure age is used, since the error with ^{26}Al exposure age is too large.
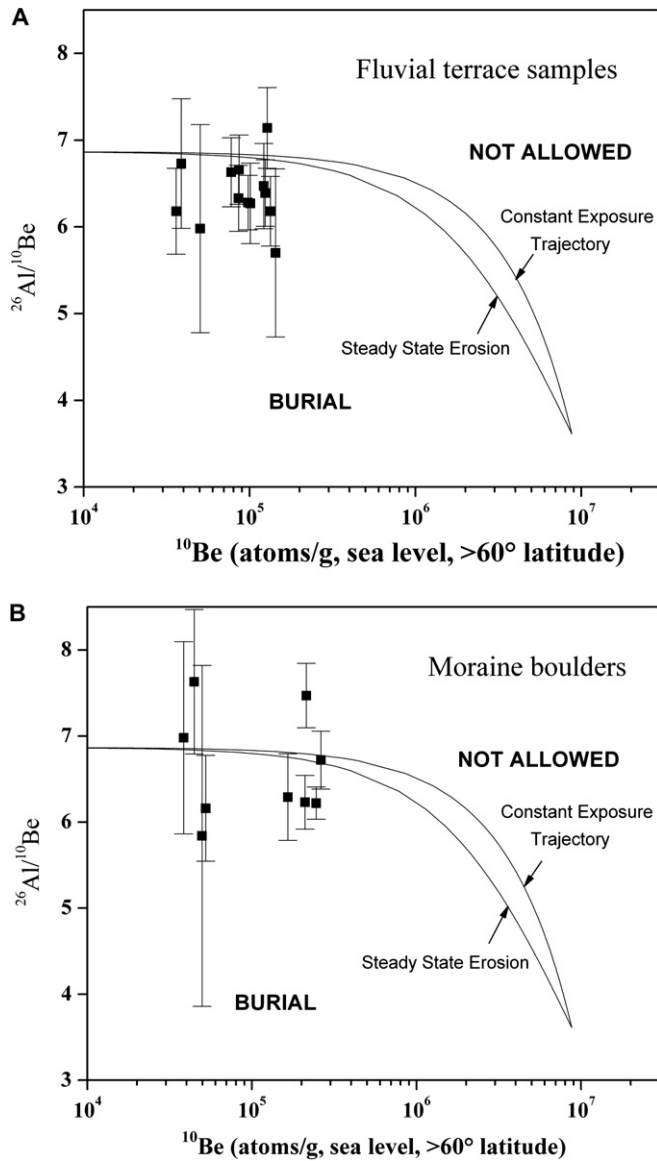
Fig. 7. Plots of $^{26}Al/^{10}Be$ ratios vs ^{10}Be concentrations for all samples. The data are basically located within the erosion island, suggesting that these samples have not experienced detectable complex exposure histories.

Fig. 8. (A) Plot of elevations vs exposure ages for the hanging wall terrace boulders. The virtually linear relationship between elevation and exposure age suggests constant downcutting of the moraine dam during drainage of the dammed lake; (B) fitting the average exposure age of the footwall terrace to the linear relationship in (A), we obtain uplift of the footwall of 130 m during 23.3 ka.

the ages suggests a long duration of the dammed lake, which appears unrealistic. Nevertheless, later re-measurements of the same samples using optical stimulated luminescence (OSL) technique give much younger ages (5.5–15 ka, unpublished data of Zhao). The problem related to the discrepancy of the ages between different techniques is unclear. The occurrences of lacustrine sediments upstream of Daju in all cases lie below 1900 m. The highest terrace at the Daju Basin within the hanging wall now sits at ~1800 m. If we assume the elevation of the moraine dam crest was originally at 1900 m, and was eroded at a rate of 7.6 m/ka by overtopping stream flow, the moraine dam then likely formed around 41 ka ago, roughly similar to the average exposure age of 47 ka we obtained for the oldest glacial remnants around the Yulong Mountains. This similarity supports our identification of the deposits at the Daju Basin as till of glacial origin.

In a tectonically rising landscape, river incision rates generally match rock uplift rates. For the Yulong Mountains and adjacent Daju Basin the situation seems a little more complicated; the
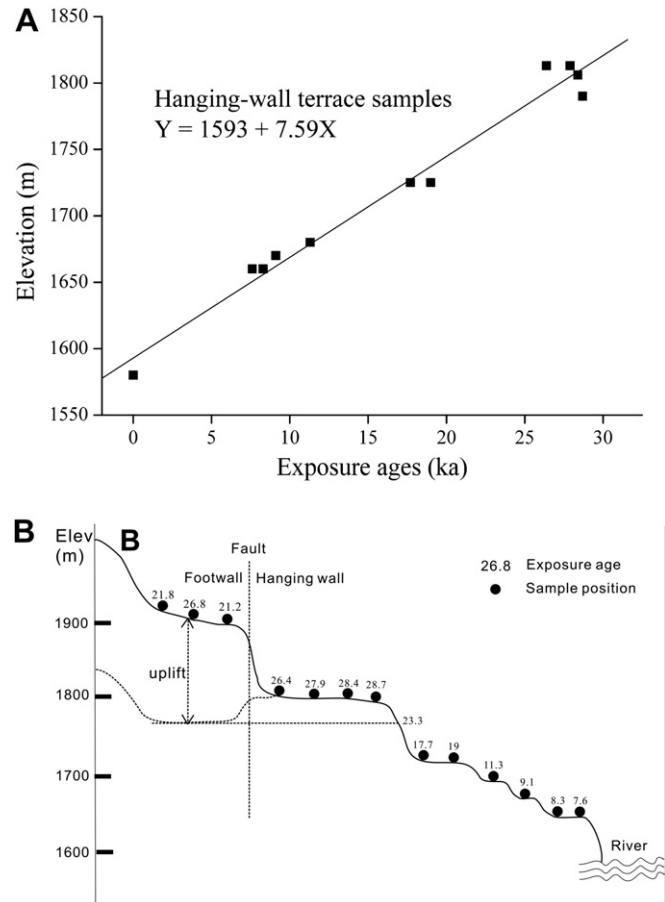
Yulong Mountains rise and the Daju Basin subsides. Thus, in normal equilibrium conditions, the river incision rate at the foot of the Yulong Mountains should be similar to the uplift rate of the mountains, which average 5.6 m/ka. At the Daju Basin the river incision rate should be <5.6 m/ka, as slope becomes smaller. The 7.6 m/ka downcutting rate of the moraine dam, which exceeds the 5.6 m/ka uplift rate, suggests that the river has not retained its pre-damming conditions. Currently the river bed at Daju has reached the limestone bedrock (Fig. 9A). We have also found old fluvial gravels at the north ferry of the Daju Basin (Fig. 9B). It appears that it takes over 10^4 years for the river to return to normal or pre-damming conditions.

The preservation of relics of the moraine dam in the current Daju Basin suggests its stability during at least the past 28 ka. The stability of moraine dams depends of their geometry, internal structure, material properties, and particle size distribution (Weidinger et al., 2002) as well as volume and rate of water and sediment inflow and seepage processes (Korup and Tweed, 2007). Costa and Schuster (1988) presented several mechanisms of dam failure. The most common failure mechanism involves overtopping by a wave or a series of waves generated by icefall or rockfall into the lake basin. Richardson and Reynolds (2000) assert that 53% of catastrophic moraine dam failures in the Himalaya are initiated by such displacement waves. Settlement and subsequent failure of moraine dams accompanying earthquakes provides another

Fig. 9. (A) Limestone bedrock appears at the river floor at the north of the Daju Basin; (B) old fluvial gravels beneath late Quaternary deposits at the northern ferry of Daju.

potential failure mechanism. Overtopping and breaching by excessive runoff during glacial retreat, snowmelt, or intense rainfall afford one more likely failure mechanism.

The Yulong Mountains upstream of the moraine dam at Daju rise with high-relief of 3800 m, and landslides often occur in this region. The Daju Basin lies in the domain of the southwest Asian monsoon. Thus enhanced precipitation driven by the southwest Asian monsoon during warm periods may lead to heavy rainfalls that likely have significant impacts on the stability of the dam. The Daju Basin also sits within a tectonically active belt, with frequent earthquakes. Despite all these factors that could trigger the sudden failure of the moraine dam, the dam at the Daju Basin has remained quite stable and with relatively constant erosion during the recent past. This suggests that the mechanism of dam failure is complicated and still not well-understood. Thus, the mechanisms of dam failure cannot be generally applied from case to case, or from one region to another (Mckillop and Clague, 2007).

As the moraine-dammed lake drained gradually during the past 10^4 years, sediments may have covered the river bed within the lake and preserved its bedorck from erosion. Because glaciation may have occurred periodically within the Yulong Mountains during the Quaternary, damming of the Jinsha River may have also occurred periodically. Erosion of the river bed west of the Yulong Mountains may not remain constant over a time-scale of 10^4 years to 10^5 years.

5.3. Past glaciations around the Yulong Mountains

This study obtained average exposure ages for the moraine boulders located in the east and west sides of the Yulong Mountains of 10.2 ka and 47 ka, respectively. These ages differ considerably from those reported by Zhao et al. (1999; 2007a), which suggested ages of 500–700 ka. One possibility for the discrepancy is that the cosmogenic nuclide exposure ages reflect exposure of moraine ridges by denudation, while the ages from Zhao et al. (1999, 2007a) record the time of moraine deposition. From the downcutting rate of the moraine-based fluvial terraces, we infer the time of moraine deposition at the Daju Basin to be of MIS-3. As this moraine ridge was deposited at below 2000 m, any moraines formed earlier on the east side of the Yulong Mountains would have been removed to similar elevations. The moraine ridges preserved in Ganhaizi and Ganheba at elevations of ∼3000 m should then postdate the moraine protruding into the Jinsha River. The 500–700 ka ages reported by Zhao et al. (1999) for the Ganhaizi and Ganheba moraines are therefore problematic.

The average exposure ages of 10.2 ka and 47 ka for moraine boulders around the Yulong Mountains correspond with times of high summer insolation in the northern hemisphere (warm periods) in the late Quaternary (Lambeck et al., 2002). Previous studies of past glaciations in southern Tibet suggest glacial advances during MIS-3 and the early Holocene, which have been attributed to high precipitation rates and increased moisture transport to high elevation accumulation areas (Owen et al., 2005). However, a recent study of moraine sequences in Nyalam, in the monsoonal Himalayas, southern Tibet (28.2°N, 86°E), show a lack of agreement between moraine ages and their stratigraphic order (Schaefer et al., 2008). The authors suggest that the ages do not reflect the time of moraine deposition, but rather than reflect moraine ridge denudation and related boulder exhumation after initial deposition of the moraines.

The average exposure age of 47 ka for the oldest moraine boulders preserved on the west side of the Yulong Mountains approximates the inferred time of moraine deposition at the Daju Basin. Therefore, the 47 ka exposure age seems most likely to reflect the deposition time of the boulders rather than denudation time.

Meter-size moraine boulders are widespread around Ganhaizi (Fig. 6C). These piedmont boulders are not likely to have been exposed later by removal of covering fine materials. Thus, the preservation of piedmont boulders around Ganhaizi suggests that glaciers extended to ∼3000 m during the early Holocene. The similarities in exposure ages and elevations for boulders at Ganhaizi (YN-62 and Y-63) and at Ganheba (YN-64 and YN-65) may imply that the exposure ages of these boulders reflect moraine deposition rather than denudation of preexisting moraines.

Mount Namcha Barwa (7782 m, 29.63°N, 95.06°E) also lies within the domain of the southwest Asian monsoon and exhibits a current snowline elevation similar to that in the Yulong Mountains. The Tsangpo River was dammed by glaciers flowing from Mount Namche Barwa during the early Holocene at an elevation of ∼3000 m (Montgomery et al., 2004). The development of glaciers in the domain of the southwest Asian monsoon at a similar time and to a similar elevation further supports our inference that the 10.2 ka exposure age reflects moraine deposition rather than denudation of existed moraines.

The expansion of glaciers around the Yulong Mountains during warm periods within the late Quaternary suggests that precipitation provides the controlling factor for glacier development in this monsoon-dominated region. Owen (2009) describes other examples of glacier development in Tibet during warm periods within the late Quaternary. Gonga Shan lies on the easternmost edge of the Tibetan Plateau in Sichuan province. Exposure ages of moraine

boulders around Gonga Shan suggest expansion of glaciers during the early Holocene (Owen et al., 2005). The upper Hunza valley (located in western Tibet, northern Pakistan), receives high precipitation of >2000 mm/year. Cosmogenic nuclide exposure dating shows an extensive glacial advance during the early stage of MIS-3 (Owen et al., 2002). Studies of glaciations on the Westerly-controlled Tianshan, northwest China, however, show a completely different pattern (Kong et al., 2009b). Glaciers there expanded during and after the last glacial maximum, reflecting a linkage with climate changes in the North Atlantic. As the Tibetan Plateau lies in the domain of both the Indian monsoon and the Westerlies, glaciations on some portions of the Plateau may show mixed or complicated patterns (Owen et al., 2005, 2008).

6. Summary and conclusions

Active Quaternary faults bound the Yulong Mountain range. These have caused uplift of the Yulong Mountains, subsidence of Daju and Lijiang basins, and deep incision of the Yulong Mountains by the Jinsha River.

Modern glaciers remain viable on the Yulong Mountains. Preserved past glacial remnants at lower elevations suggest glacial advances during the late Quaternary. A ridge of moraine protruded into the Jinsha River at the Daju Basin, and dammed the river. Erosion of the dam by stream flow left moraine-based fluvial terraces.

With cosmogenic nuclide ^{10}Be and ^{26}Al, we have dated the fluvial terraces at the Daju Basin and moraine boulders on the east and west sides of the Yulong Mountains. The exposure ages of the terraces range from 29 ka to 8 ka and indicate a downcutting rate of 7.6 m/ka. The preservation of the relic moraine dam over 10^4 years suggests relative stability of the moraine dam and gradual erosion of the dam on the river floor, despite the dam being located in a tectonically active belt with frequent earthquakes and adjacent to a high-relief mountain range; both of which could be major triggers of sudden failure of the moraine dam.

A terrace sits on the footwall of the Daju normal fault. By comparison with other terraces in the hanging wall, we obtained a vertical offset of 130 m for the footwall terrace during the past 23.3 ka. This gives a dip-slip rate of 5.6 m/ka for the Daju fault. Comparison with previously published slip rates for the fault for longer periods suggests increasing tectonic displacement on the Daju fault with time.

The dated moraine boulders preserved in the east and west sides of the Yulong Mountains have exposure ages of 10.2 ka and 47 ka, respectively. These ages coincide with warm periods in the late Quaternary. We believe that these ages reflect the deposition time of the moraine ridges, rather than denudation time of older moraines. The expansion of glaciers around the Yulong Mountains, within the domain of the southwest Asian monsoon, during warm periods suggests that precipitation provides the major control for glaciation in this monsoon-influenced region.

References

Baker, V.R., Benito, G., Rudoy, A.N., 1993. Paleohydrology of late Pleistocene super-flooding, Altay Mountains, Siberia. Science 259, 348–350.

Burbank, D.W., Leland, J., Fielding, E., Anderson, R.S., Brozovic, N., Reid, M.R., Duncan, C., 1996. Bedrock incision, rock uplift and threshold hillslopes in the northwestern Himalayas. Nature 379, 505–510.

Costa, J.E., Schuster, R.L., 1988. The formation and failure of natural dams. Geological Society of America Bulletin 100, 1054–1068.

Desilets, D., Zreda, M., Prabu, T., 2006. Extended scaling factors for in situ cosmogenic nuclides: new measurements at low latitude. Earth and Planetary Science Letters 246, 265–276.

Dunai, T., 2000. Scaling factors for production rates of in situ produced cosmogenic nuclides: a critical reevaluation. Earth and Planetary Science Letters 193, 197–212.

Dunai, T.J., 2001. Influence of secular variation of the geomagnetic field on production rates of in situ produced cosmogenic nuclides. Earth and Planetary Science Letters 193, 197–212.

Dunne, J., Elmore, D., Muzikar, P., 1999. Scaling factors for the rates of production of cosmogenic nuclides for geometric shielding and attenuation at depth on sloped surfaces. Geomorphology 27, 3–11.

Fan, C., Wang, G., Wang, S., Wang, E., 2006. Structural interpretation of extensional deformation along the Dali fault system, southeastern Margin of the Tibetan Plateau. International Geology Review 48, 287–310.

Fink, D., Smith, A.M., 2007. An inter-comparison of ^{10}Be and ^{26}Al AMS reference standards and the ^{10}Be half-life. Nuclear Instruments and Methods in Physics Research B 259, 600–609.

Han, Z., Guo, S., Xiang, H., Zhang, J., Ran, Y., 2004. Seismotectonic environment of occurring the February 3, 1996 M = 7.0 earthquake, Yunnan province. Acta Seismologica Sinica 17, 453–463.

He, Y., Yao, T., Theakstone, W.H., Cheng, G., Yang, M., Chen, T., 2002. Recent climatic significance of chemical signals in a shallow firn core from an alpine glacier in the South-Asia monsoon region. Journal of Asian Earth Science 20, 289–296.

Huang, P., 1960. Discussing the Yunnan geomorphological research. Quaternaria Sinica 3, 39–55 (in Chinese).

Ives, J.D., Zhang, Y., 1993. Glaciation of the Yulongxueshan, north-western Yunnan Province, People's Republic of China. Erdkunde 47, 94–104.

Jen, M.N., 1958. The glaciation of Yulong-shan in China. Erdkunde 12, 308–313.

Kaplan, M.R., Douglass, D.C., Singer, B.S., Ackert, R.P., Caffee, M.W., 2005. Cosmogenic nuclide chronology of pre-last glacial maximum moraines at Lago Buenos Aires, 46°S, Argentina. Quaternary Research 63, 301–315.

Kohl, C.P., Nishiizumi, K., 1992. Chemical isolation of quartz for measurement of in-situ-produced cosmogenic nuclides. Geochimica et Cosmochimica Acta 56, 3583–3587.

Komatsu, G., Arzhannikov, S.G., Gillespie, A.R., Burke, R.M., Miyamoto, H., Baker, V.R., 2009. Quaternary paleolake formation and cataclysmic flooding along the upper Yenisei River. Geomorphology 104, 143–164.

Kong, P., Na, C., Fink, D., Ding, L., Huang, F., 2007. Erosion in northwest Tibet from In-situ-produced cosmogenic ^{10}Be and ^{26}Al in bedrock. Earth Surface Processes and landforms 32, 116–125.

Kong, P., Granger, D.E., Wu, F., Caffee, M.W., Wang, Y., Zhao, X., Zheng, Y., 2009a. Cosmogenic nuclide burial ages and provenance of the Xigeda paleo-lake: implications for evolution of the Middle Yangtze River. Earth and Planetary Science Letters 278, 131–141.

Kong, P., Fink, D., Na, C., Huang, F., 2009b. Late Quaternary glaciation of the Tian-shan, Central Asia, using Cosmogenic ^{10}Be surface exposure dating. Quaternary Research 72, 229–233.

Korup, O., Montgomery, D.R., 2008. Tibetan plateau river incision inhibited by glacial stabilization of the Tsangpo gorge. Nature 455, 786–790.

Korup, O., Tweed, F., 2007. Ice, moraine, and landslide dams in mountainous terrain. Quaternary Science Reviews 26, 3406–3422.

Lacassin, R., Schärer, U., Hervé Leloup, P., Arnaud, N., Tapponnier, P., Liu, X., Zhang, L., 1996. Tertiary deformation and metamorphism SE of Tibet: the folded Tiger-leap décollément of NW Yunnan, China. Tectonics 15, 605–622.

Lal, D., 1991. Cosmic ray labeling of erosion surfaces: in situ production rates and erosion models. Earth Planetary Science Letters 104, 424–439.

Lambeck, K., Esat, T., Potter, E.K., 2002. Links between climate and sea levels for the past three million years. Nature 419, 199–206.

Leland, J., Reid, M.R., Burbank, D.W., Finkel, R., Caffee, M., 1998. Incision and differential bedrock uplift along the Indus River near Nanga Parbat, Pakistan Himalaya, from ^{10}Be and ^{26}Al exposure age dating of bedrock straths. Earth and Planetary Science Letters 154, 93–107.

Lifton, N., Bieber, J., Clem, J., Duldig, M., Evenson, P., Humble, J., Pyle, R., 2005. Addressing solar modulation and long-term uncertainties in scaling secondary cosmic rays for in situ cosmogenic nuclide applications. Earth and Planetary Science Letters 239, 140–161.

Liu, H., Hu, R., Zeng, R., 2005. Analysis of the basic features and the formation mechanism of Liangjiaren loose deposits in Tiger-Leaping-Gorge, Yunnan. Quaternary Sciences 25, 100–106 (in Chinese).

Ma, R., Peng, J., 2006. Discussion on relationship between earthquake magnitude, repture scale and displacement. Journal of Northwest University 36, 799–803 (in Chinese).

McKillop, R.J., Clague, J.J., 2007. Statistical, remote sensing-based approach for estimating the probability of catastrophic drainage from moraine-dammed lakes in southwestern British Columbia. Global and Planetary Change 56, 153–171.

Montgomery, D.R., Hallet, B., Liu, Y., Finnegan, N., Anders, A., Gillespie, A., Greenbery, H.M., 2004. Evidence for Holocene megafloods down the Tsangpo River gorge, southeastern Tibet. Quaternary Research 62, 201–207.

Ming, Q., 1996. The Quaternary glaciation in Yu-Long mountains. Journal of Yunnan Normal University 16, 94–104 (in Chinese).

Ning, B., He, Y., He, X., Pang, H., Yuan, L., Zhao, J., Lu, A., Song, B., 2006. Potential impacts of glacier retreating of the Mt. Yulong on the socioeconomic development in Lijiang city. Journal of Glaciology and Geocryology 28, 885–892 (in Chinese).

Nishiizumi, K., Imamura, M., Caffee, M.W., Southon, J.R., Finkel, R.C., McAninch, J., 2007. Absolute calibration of [10]Be AMS standards. Nuclear Instruments and Methods in Physics Research B 258, 403–413.

Owen, L.A., 2009. Latest Pleistocene and Holocene glacier fluctuations in the Himalaya and Tibet. Quaternary Science Reviews 28, 2150–2164.

Owen, L.A., Finkel, R.C., Caffee, M.W., Gualtieri, L., 2002. Timing of multiple late Quaternary glaciations in the Hunza Valley, Karakoram Mountains, northern Pakistan: defined by cosmogenic radionuclide dating of moraines. Geological Society of America Bulletin 114, 593–604.

Owen, L.A., Finkel, R.C., Barnard, P.L., Ma, H., Asahi, K., Caffee, M.W., Derbyshire, E., 2005. Climatic and topographic controls on the style and timing of Late Quaternary glaciation throughout Tibet and the Himalayas defined by [10]Be cosmogenic radionuclide surface exposure dating. Quaternary Science Reviews 24, 1391–1411.

Owen, L.A., Caffee, M.W., Finkel, R.C., Seong, B.Y., 2008. Quaternary glaciations of the Himalayan–Tibetan orogen. Journal of Quaternary Science 23, 513–532.

Pang, H., He, Y., Lu, A., Zhao, J., Ning, B., Yuan, L., Song, B., Zhang, N., 2006. Comparisons of stable isotopic fractionation in winter and summer at Baishui Glacier No. 1, Mt. Yulong, China. Journal of Geographical Sciences 16, 306–314.

Putkonen, J., Swanson, T., 2003. Accuracy of cosmogenic ages for moraines. Quaternary Research 59, 255–261.

Reuther, A.U., Herget, J., Ivy-Ochs, S., Borodavko, P., Kubik, P.W., Heine, K., 2006. Constraining the timing of the most recent cataclysmic flood event from ice-dammed lakes in the Russian Altai Mountains, Siberia, using cosmogenic in situ [10]Be. Geology 34, 913–916.

Richardson, S.D., Reynolds, J.M., 2000. An overview of glacial hazards in the Himalayas. Quaternary International 65/66, 31–47.

Riebe, C.S., Kirchner, J.W., Granger, D.E., Finkel, R.C., 2001. Minimal climatic control on erosion rates in the Sierra Nevada, California. Geological Society of America 29, 447–450.

Saito, Y., Yang, Z., Hori, K., 2001. The Huanghe (Yellow River) and Changjiang (Yangtze River) deltas: a review on their characteristics, evolution and sediment discharge during the Holocene. Geomorphology 41, 219–231.

Schaefer, J.M., Oberholzer, P., Zhao, Z., Ivy-Ochs, S., Wieler, R., Baur, H., Kubik, P.W., Schlüchter, C., 2008. Cosmogenic beryllium-10 and neon-21dating of late Pleistocene glaciations in Nyalam, monsoonal Himalayas. Quaternary Science Reviews 27, 295–311.

Stone, J.O., 2000. Air pressure and cosmogenic isotope production. Journal of Geophysical Research 105, 23753–23759.

Weidinger, J.T., Wang, J.D., Ma, N.X., 2002. The earthquake-triggered rock avalanche of Cui Hua, Qin Ling Mountains, P.R. China-the benefits of a lake-damming prehistoric natural disaster. Quaternary International 93/94, 207–214.

Wu, Z., Zhang, Y., Hu, D., Zhao, X., Ye, P., 2008. Late Quaternary normal faulting and its dynamic mechanism of the Haba-Yulong east piedmont, northwest Yunnan. Science in China D 38, 1361–1375.

Xiao, H., Shen, J., Xiao, X., 2006. Paleoenvironmental evolution of Heqing basin in Yunnan Province since 2.78 Ma. Journal of Lake Science 18, 255–260 (in Chinese).

Xiao, X., Shen, J., Wang, S., Xiao, H., Tong, G., 2007. Palynological evidence for vegetational and climatic changes from the HQ deep drilling core in Yunnan Province, China. Science in China D 50, 1189–1201.

Zhang, Z., He, Y., Pang, H., 2004. Variation of glaciers in response to ENSO in the mount Yulong. Journal of Glaciology and Geocryology 26, 294–297 (in Chinese).

Zhang, N., He, Y., He, X., Pang, H., Zhao, J., 2007. The analysis of icefall at Mt. Yulong. Journal of Mountain Science 25, 412–418.

Zhao, X., Qu, Y., Li, T., 1999. Pleistocene glaciations along the eastern foot of the Yulong mountains. Journal of Glaciology and Geocryology 21, 242–248 (in Chinese).

Zhao, X., Zhang, Y., Qu, Y., Guo, C., 2007a. Pleistocene glaciations along the western foot of the Yulong mountains and their relationship with the formation and development of the Jinsha river. Quaternary Sciences 27, 35–55 (in Chinese).

Zhao, X., Qu, Y., Zhang, Y., Hu, D., Guo, C., 2007b. Discovery of Shigu paleolake in the Lijiang area, northwestern Yunnan, China and its significance for the development of the modern Jinsha River valley. Geological Bulletin of China 26, 960–969.

Zheng, B., 2000. Quaternary glaciations and glacier evolution in the Yulong Mount, Yunnan. Journal of Glaciology and Geocryology 21, 242–248 (in Chinese).